# Large-scale seroepidemiology uncovers nephro-urological pathologies in persons with tau autoimmunity

**Authors:**

Andreia D. Magalhães[1†], Marc Emmenegger[1&], Elena De Cecco[1], Manfredi Carta[1‡], Karl Frontzek[1], Andra Chincisan[1‖], Jingjing Guo[1], Simone Hornemann[1*], Adriano Aguzzi[1*]

**Affiliations:**

[1]Institute of Neuropathology, University of Zurich; CH-8091 Zurich, Switzerland

[†] Present address: Department of Neurology, Inselspital, Bern University Hospital; CH-3010 Bern, Switzerland

[&]Present address: Division of Medical Immunology, Department of Laboratory Medicine, University Hospital Basel; CH-4031 Basel, Switzerland

[‡]Present address: Institute of Neurology, University of Zurich; CH-8091 Zurich, Switzerland

§ Present address: University College London, Institute of Neurology, Queen Square Brain Bank; WC1N 1PJ London, United Kingdom

[‖] Present address: Credit Suisse; CH-8001 Zurich, Switzerland

[*]Correspondence: Simone Hornemann and Adriano Aguzzi

Institute of Neuropathology, University of Zurich; CH-8091 Zurich, Switzerland

Phone: 0041 44 255 2107

Simone.hornemann@uzh.ch and adriano.aguzzi@uzh.ch

**Running title:** Anti-tau autoantibodies

**Competing interests:**

The authors declare that they have no conflict of interest.

**Abstract:**

Intraneuronal aggregates of the microtubule-associated protein tau play a pivotal role in Alzheimer's disease and several other neurodegenerative syndromes. Anti-tau antibodies can reduce pathology in mouse models of neurodegeneration and are currently tested in humans. Here, we performed a large-scale seroepidemiological search for anti-tau IgG autoantibodies (ατ) on 40,497 human plasma samples. High-titer $\alpha\tau^+$ individuals were surprisingly prevalent, with hospital patients being three times more likely to be $\alpha\tau^+$ ($EC_{50} \geq 2^6$; a nominal dilution of > 1/64) than healthy blood donors (4.8% vs 1.6%). The prevalence increased with age over 70 years-old (RR 1.26, 95%CI 1.11-1.43, P<0.001) and was higher for women (RR 1.20, 95%CI 1.07-1.39, P=0.002). The autoantibodies bound selectively to tau, inhibited tau aggregation *in vitro*, and interfered with tau detection in plasma samples. No association was found between ατ autoantibodies and neurological disorders. Instead, tau autoreactivity showed a significant association with kidney and urinary disorders (adjusted RR 1.27, 95%CI 1.10-1.45, P=0.001 and 1.40, 95%CI 1.20-1.63, P<0.001, respectively). These results suggest a previously unrecognized association between ατ autoimmunity and extraneural diseases.

44 **Main Text:**

45 **INTRODUCTION**

46 Tau is a microtubule binding protein involved in cytoskeletal dynamics and expressed in neurons
47 (1, 2) and in extraneural tissues, including kindey (1-5). It plays a pivotal role in a variety of neu-
48 rodegenerative diseases, including Alzheimer's disease (AD) (6), progressive supranuclear palsy,
49 and various syndromes collectively referred to as tauopathies (7). The presence of brain neurofi-
50 brillary tau tangles correlates with cognitive decline (8), and plasma measurements of total and
51 phosphorylated tau have emerged as promising biomarkers for the detection and monitoring of AD
52 progression (9-12). Moreover, active and passive immunization with antibodies against a wide
53 range of tau epitopes can reduce pathology and functional decline in animal models of tauopathies
54 (13, 14) and are being tested in clinical trials of neurodegenerative diseases (15).

55 Natural autoantibodies are immunoglobulins generated against self-antigens in the absence of ex-
56 ternal antigen stimulation (16). They are a normal part of the immunoglobulin repertoire and have
57 physiological roles in homeostasis and surveillance, including the clearance of cellular debris, anti-
58 inflammatory activity, and first-line defense against pathogens (17). However, in certain situations,
59 natural autoantibodies can also cause pathological autoimmunity. The distinction between home-
60 ostatic and pathological autoantibodies is sometimes unclear and may depend on an individual's
61 physiological state (18). The study of natural autoantibodies can therefore inform about properties
62 of their targets, e.g. unrecognized protective or contributing roles in disease (19). Some natural
63 autoantibodies can cause neurological disorders, such as antibodies targeting the N-methyl-D-as-
64 partate receptor (NMDAR) in encephalitis (20) or antibodies targeting aquaporin-4 (AQP4) in
65 neuromyelitis optica (21). Conversely, natural antibodies against amyloid-β have been suggested

66 to protect and slow the progression of AD; aducanumab, a monoclonal antibody developed from
67 B-cells of cognitively normal older age individuals, has been studied as a treatment for AD (22).
68 Anti-tau autoantibodies have been detected in plasma of patients with AD (23) and Parkinson's
69 disease (24), but also in non-neurodegeneration controls (23). The effects, if any, of natural anti-
70 tau autoantibodies in modulating the risk of developing neurodegenerative diseases are unknown.
71 The study of individuals with anti-tau autoantibodies could clarify their potential as modifiers or
72 biomarkers of disease. Here, we tested 40,497 plasma samples from healthy blood donors and from
73 patients admitted to a university hospital in the frame of a two-sites cross-sectional study. We
74 found that anti-tau autoimmunity is highly specific and surprisingly frequent, with its prevalence
75 increasing with age. Unexpectedly, natural anti-tau autoantibodies were associated with a previ-
76 ously unrecognized syndrome comprising kidney and urinary disorders.

77 **RESULTS**

78 **Prevalence of naturally occurring plasma anti-tau autoantibodies**

79 We designed a cross-sectional study to investigate naturally occurring plasma IgG autoantibodies
80 against the microtubule binding domain of tau protein (MTBD-tau) corresponding to the human
81 truncated 4R-tau (residues 244–372 relative to 2N4R human tau). Plasma samples from 32,291
82 university hospital patients (age ≥ 18 years) and 8,206 healthy blood donors were screened by
83 miniaturized Enzyme-Linked Immunosorbent Assay (ELISA, Figure 1A) (25-27).

84 We excluded 7,952 and 1,616 non-informative samples from patients and blood donors, respec-
85 tively (fitting error >20% $-\log_{10}(EC_{50})$ or high background), and analyzed 24,339 patient samples
86 and 6,590 healthy blood-donor samples (Figure 1A). A titer of $-\log_{10}(EC_{50}) \geq 1.8$, approximately
87 corresponding to a nominal dilution of > 1/64 or an $EC_{50} \geq 2^6$, was empirically selected as a cutoff
88 to call tau-autoreactive samples (henceforth named $\alpha\tau^+$) (25). This threshold represents the inflec-
89 tion point in our serial dilution assays above background and below saturation and was chosen to
90 best balance sensitivity and specificity.1,169 hospital samples (4.80%) but only 104 healthy donor
91 samples (1.58%) were $\alpha\tau^+$ (Figure 1A-C). Hence, anti-tau immunoreactivity was more prevalent
92 in unselected hospital patients than in healthy individuals (P<0.001). Demographic data was avail-
93 able for 4,157 of the 6,590 blood donors. Median ages were 42 (IQR 29-54) and 55 years (IQR:
94 40-69) for healthy donors and hospital patients, respectively (P<0.001). Of the healthy blood do-
95 nors, 40.9% (n=1,698) were women, whereas for the hospital group, 47.7% (n=11,609) of the
96 patients were women (P<0.001). Multivariate log-binomial regression (28, 29) adjusted for age
97 and sex showed that hospital patients had a 2.3x higher risk than healthy donors to be $\alpha\tau^+$ (aRR
98 2.30, 95%CI 1.83-2.92, P<0.001, Figure 1D).

99 The replicability of the microELISA screen was found to be high ($R^2$=0.84, P<0.001, Figure 1E).
100 There was no cross-reactivity to two other proteins implicated in neurodegeneration, amyloid-ß
101 pyroglutamate and the cellular prion protein ($PrP^C$) (27). Of 12,297 patient samples, 604 samples
102 were positive against MTBD-tau and 5 against amyloid-ß pyroglutamate but none was cross-reac-
103 tive against both targets (P=1, $\chi^2$ test) (Figure 1F), Moreover, of 13,099 patient samples, 694 were
104 reactive against MTBD-tau and 15 against $PrP^C$, but again none was cross-reactive against both
105 targets (P=0.734, $\chi^2$ test) (Figure 1G).
106
107 **Specificity and biological activity of $\alpha\tau^+$ samples**
108 To investigate their specificity, we purified anti-tau autoantibodies by MTBD-tau affinity chroma-
109 tography from four individual $\alpha\tau^+$ patients (P1-P4) and from a pool of six $\alpha\tau^+$ sample (patient_IDs:
110 J909190817, J802220975, J909190382, J90806029, J908060881 and J805040458). Purified anti-
111 MTBD-tau autoantibody samples had $EC_{50}$ values of 0.042-14.45 µg/ml whereas the mouse anti-
112 MTBD-tau antibody RD4 (30) had $EC_{50}$=0.002 µg/ml (Figure 2A). In a soluble-competition im-
113 munoassay (Figure 2B), purified $\alpha\tau^+$ autoantibodies showed a concentration-dependent binding to
114 recombinant MTBD-tau purified by cation exchange and size exclusion chromatography and to a
115 pool of 8 synthetic MTBD-tau peptides but not to albumin or an unrelated synthetic peptide (Figure
116 2C). To probe for polyreactivity, purified $\alpha\tau^+$ autoantibodies were tested against several structur-
117 ally unrelated autoantigens and bacterial proteins, including MTBD-tau, albumin, cardiolipin,
118 DNA, insulin, and lipopolysaccharides (LPS). Anti-tau autoantibodies were reactive against
119 MTBD-tau but not against any of the other antigens or uncoated plates (Figure 2D).
120 In immunofluorescent stainings, purified ατ autoantibodies co-localized to cytoplasmic EGFP-
121 0N4RTau in SH-SY5Y cells and showed similar binding patterns to an anti-tau mouse monoclonal

122 antibody H7, but not to non-transfected cells (Figure 2E). On western blots, purified ατ autoanti-
123 bodies detected tau-specific bands in cell lysates of SH-SY5Y cells overexpressing $tau^{P301L/S320F}$,
124 but not in parental (wt) SH-SY5Y cells (Figure 2F and Supplemental Figure 1). Hence, the immu-
125 noreactivity of $\alpha\tau^{+}$ samples was highly specific for tau. All IgG subclasses and both κ and λ light
126 chains were present in $\alpha\tau^{+}$ patients' samples (Figure 2G and H). Epitope mapping and light-chain
127 typing revealed a polytypic response in at least 8 out of the 13 $\alpha\tau^{+}$ samples (Figure 2H and I).
128 To investigate whether purified $\alpha\tau^{+}$ autoantibodies interfere with the aggregation of MTBD-tau,
129 samples from patients P7 and P8 were tested in an *in vitro* tau aggregation assay (31). MTBD-tau
130 aggregation was induced by heparin and shaking and monitored using Thioflavin T (ThT; Figure
131 3A). The presence of $\alpha\tau^{+}$ autoantibodies reduced the plateau of the ThT fluorescence signal in the
132 kinetic trace by about half, whereas antibodies purified by protein G affinity chromatography from
133 an $\alpha\tau^{-}$ patient had no effect (Figure 3A). Hence, $\alpha\tau^{+}$ autoantibodies were able to specifically bind
134 to and inhibit MTBD-tau aggregation *in vitro*.
135 Plasma tau is a promising biomarker of progression for several neurological diseases (9-12, 32).
136 We examined the effects of ατ autoantibodies onto the performance of plasma tau immunoassays
137 (Figure 3B). Purified ατ autoantibodies from 5 patients (P2-P6) were added to $tau^{441}$-spiked
138 plasma. After incubation, the amount of free $tau^{441}$ was analyzed by ELISA using commercial anti-
139 tau antibodies for capture (BT2, epitope on human $tau^{441}$: residues 194-198) and detection
140 (ab64193, epitope on non-phosphorylated and phosphorylated human $tau^{441}$ surrounding residue
141 262) (33). Purified ατ autoantibodies P4-P6 induced a concentration-dependent impairment of de-
142 tection of $tau^{441}$ hampering the detection of plasma-spiked $tau^{441}$ by approximately tenfold at
143 higher anti-MTBD-tau autoantibody concentration (Figure 3C and D). In contrast, P2-P3 did not

144 show any significant impairment of the detection of plasma-spiked tau$^{441}$. This variability of inter-
145 ference is explained by the binding epitopes on tau$^{441}$. P4-P6 occupy tau residues 244 to 282 in-
146 cluding the binding epitope of ab64193, whereas P2-P3 occupy residues 273 to 327 which are
147 outside the epitope of ab64193 (Figure 3C and D and Supplemental Figure 2). Hence, the presence
148 of $\alpha\tau^+$ autoantibodies can interfere with the detection of plasma tau in immunoassays depending
149 on the combination of epitopes of the patient samples and of commercial antibodies used in im-
150 munoassays.
151
152 **Demographic characteristics of tau-immunoreactive patients**
153 The age of $\alpha\tau^+$ patients (median: 58 years; IQR: 43-71) was significantly higher than that of $\alpha\tau^-$
154 (median: 55; IQR: 40-68; $P < 0.001$, Figure 4A). Univariate logistic regression analyses of health
155 records for the 24,339 hospital patients showed that the prevalence of $\alpha\tau$ immunoreactivity in-
156 creased with age, from 3.9% in patients aged <29 years to 7.6% in patients aged >90 years
157 ($P<0.001$, Figure 4B). A log-binomial regression model (28, 29) estimated that the RR for the
158 presence of anti-MTBD-tau autoantibodies was highest for patients aged 70-99 years (RR 1.26,
159 95% CI 1.11-1.43, $P<0.001$, Figure 4C) and for women (RR 1.20, 95% CI 1.07-1.39, $P=0.002$,
160 Figure 4C). Due to the association of anti-MTBD-tau autoantibodies with increased age and female
161 sex, all further RRs were calculated using a multivariate log-binomial regression model adjusted
162 for age and sex. To identify potential correlations between $\alpha\tau^+$ and specific diseases, we analyzed
163 the admission to clinical departments. The highest RRs for $\alpha\tau^+$ were found for angiology (aRR
164 1.84, 95% CI 1.21-2.63, $P=0.002$) and nephrology (aRR 1.50, 95% CI 1.16-1.89, $P=0.001$, Figure
165 4D-E), whereas no significant difference was found between the percentage of $\alpha\tau^+$ and $\alpha\tau^-$ patients
166 from the department of neurology (Figure 4D).

167

168 **Neurological disorders and anti-tau autoimmunity**

169 We next mined pseudonymized clinical diagnoses from the clinical records of the USZ pertaining
170 to the diagnoses of 23,375 patients as represented by ICD-10 codes (Figure 5A). Given the in-
171 volvement of tau in neurodegenerative diseases (6), we focused on evaluating the association be-
172 tween anti-MTBD-tau autoantibodies and neurological diseases, which we categorized in 23 main
173 groups of disorders. No associations between $\alpha\tau^+$ and neurological diseases were identified (Figure
174 5A). We further performed a targeted screen using plasma samples from 47 patients with AD and
175 68 similarly aged non-AD patients selected from our plasma biobank (median age of AD patients
176 78 years, IQR 70,5-86, and median age of control patients 81 years, IQR 71-85, Supplemental
177 Table 1). Samples were tested for anti-MTBD-tau IgG autoantibodies, as in the primary screen,
178 and additionally for anti-MTBD-tau IgA autoantibodies and anti-full-length-tau (tau441) IgG and
179 IgA autoantibodies. No significant difference in reactivity was observed between the plasma sam-
180 ples from AD patients and non-AD controls in this small convenience cohort (Figure 5B), which
181 is in line with the previous finding that the presence of autoantibodies targeting MTBD-tau is
182 unrelated to AD or other neurological disorders.

183

184 **Systemic disorders and anti-tau autoimmunity**

185 We next assessed possible associations between tau autoimmunity and extraneural diseases, which
186 we binned into 27 main groups of disorders (Figure 6A). After adjustment for multiple compari-
187 sons, $\alpha\tau$ immunoreactivity showed significant associations with vascular disorders (aRR 1.51, 95%
188 CI 1.28-1.77, P<0.001), nutritional disorders (aRR 1.31, 95% CI 1.14-1.50, P<0.001), anemia
189 (aRR 1.49, 95% CI 1.21-1.82, P<0.001), kidney disorders (aRR 1.27, 95% CI 1.10-1.45, P=0.001)

190 and urinary disorders (aRR 1.40, 95%CI 1.20-1.63, P<0.001) (Figure 6A), whereas no association
191 was observed among patients with autoimmune disorders (Supplemental Figure 3). There was no
192 difference in the coincidence of all comorbidities between $\alpha\tau^+$ samples (5, 0.46%) and $\alpha\tau^-$ samples
193 (69, 0.33%) (P=0.633).
194 To address potential biases arising from grouping and selecting major categories, we explored the
195 association between $\alpha\tau^+$ and individual ICD-10 codes. Across 276 individual ICD-10 codes and
196 after correction for multiple comparisons, eight exhibited significant associations with $\alpha\tau^+$ (Figures
197 6B and C). These included "E61–deficiency of other nutrient elements" (aRR 2.22, 95% CI 1.54-
198 3.06, P<0.001), "I74–arterial embolism and thrombosis" (aRR 2.09, 95% CI 1.40-2.94, P<0.001),
199 "N30–cystitis" (aRR 1.84, 95% CI 1.32-2.47, P<0.001), "I70–atherosclerosis" (aRR 1.57, 95% CI
200 1.29-1.89, P<0.001), "D50–iron deficiency anemia" (aRR 1.50, 95% CI 1.21-1.82, P<0.001),
201 "N39–other urinary disorders" (aRR 1.40, 95% CI 1.19-1.64, P<0.001), "B96–other bacterial
202 agents as the cause of diseases" (aRR 1.40, 95% CI 1.17-1.66, P<0.001) and "N18–chronic kidney
203 disease" (aRR 1.38, 95% CI 1.18-1.60, P<0.001; Figure 6C). Conversely, we found no significant
204 negative association between tau autoreactivity and any ICD-10 codes that could suggest a de-
205 creased risk for a specific disease in $\alpha\tau^+$ patients (Figure 6C). To verify relevant associations, we
206 used Bayesian logistic regression using logit-transformed $EC_{50}$ values (-logit[$EC_{50}$]) as a continu-
207 ous outcome. All the previously referred eight ICD-10 codes showed positive associations with -
208 logit[$EC_{50}$] (Figure 6D).
209 To validate these conditions as significant associations with plasma MTBD-tau IgG autoantibod-
210 ies, we examined the association between $\alpha\tau^+$ and 106 commonly requested laboratory parameters
211 (Supplemental Table 2) using data available for 24,177 patients, independently of any ICD-10
212 classifiers. After correction for multiple comparisons, the laboratory markers "Leukocytes, urine",

213 “Potassium” and “Urea” were positively associated with tau autoimmunity (Figure 6E). The asso-
214 ciation with increasing levels of urea and potassium suggests a link to kidney failure, whereas
215 leukocytes in urine are a feature of urinary tract infections. These findings support the hypothesis
216 that anti-tau autoimmunity correlates with such disorders. Accordingly, the prevalence of chronic
217 kidney disease was 12.4% in $\alpha\tau^-$ and 17.7% in $\alpha\tau^+$ patients, whereas that of other urinary disorders
218 was 10.3% in $\alpha\tau^-$ and 15.1% in $\alpha\tau^+$ patients (Figure 6F).
219

220 **DISCUSSION**

221 This study was designed to discover novel associations between autoreactivity to tau and human
222 diseases. This approach of “reverse immunopathology” is hypothesis-free: it does not pose con-
223 straints on the type of diseases that might result from anti-tau immunity. While the approach is
224 generally applicable to any autoantigen, its predictive power relies on the analysis of large patient
225 collectives, which in turn requires the development of high-throughput methods at reasonable cost.
226 We therefore miniaturized antibody detection to 3 µl/sample in 1,536-well microplates, allowing
227 to run 40,000 assays/24 hrs with minimal hands-on time. We performed >300,000 immunoassays
228 on >40,000 plasma samples for ατ autoreactivity. Each sample was measured at eight dilution
229 points, enabling precise and unambiguous titer determinations (25-27).
230 Plasma ατ IgG were more prevalent in women and increased with age, reaching 7.6% in the cohort
231 of 90-99-year-olds. The specificity of $\alpha\tau^+$ plasma to MTBD-tau was high and was confirmed by
232 multiple assays including epitope mapping. The age- and sex-adjusted $\alpha\tau^+$ rate in hospital patients
233 was three-fold higher than in healthy blood donors and considerably exceeded the previously re-
234 ported seroprevalences of autoantibodies targeting other intracellular neuronal targets (0.4% and
235 2%) (34), suggesting a potential correlation with disease states (34).

236 However, we did not find any association between $\alpha\tau^+$ and any neurological conditions including
237 neurodegenerative diseases using both ICD-10 classification as well as a convenience AD and
238 non-AD cohort of plasma samples, corroborating with reports of similar levels of plasma tau au-
239 toantibodies in AD patients and non-demented controls (35). Instead, we uncovered a robust, spe-
240 cific association between $\alpha\tau^+$ positivity and kidney and urinary disorders. This was independently
241 validated by associations with higher prevalence of positive samples from the department of Neph-
242 rology, grouped kidney and urinary diseases, individual kidney and urinary diagnosis codes and
243 related clinical laboratory biomarkers, such as high serum urea and potassium and high urine leu-
244 kocytes.
245 Seroepidemiological studies cannot establish causality: $\alpha\tau$ seropositivity could be a cause or a
246 consequence of the clinical syndromes associated with it (36). Therefore, due to its design, this
247 study cannot conclude on the homeostatic or pathological role of the anti-tau IgG autoantibodies
248 identified in the plasma of patients and healthy blood donors. However, tau is expressed in ex-
249 traneural tissues, including kidney podocytes and urinary bladder (2-5), and its ablation causes
250 glomerular pathologies (37).
251 These findings raise the possibility that plasma $\alpha\tau$ autoantibodies might drive kidney and/or uro-
252 logical pathologies. Alternatively, they could reflect a physiological autoimmunity with low affin-
253 ity autoantibodies playing a role in immune surveillance and the clearance of debris. Another pos-
254 sibility is that an underlying pathological process causing renal/bladder tissue injury and inflam-
255 mation, may lead to the extracellular release of intracellular proteins, including tau. Damage to
256 tubular epithelial cells or glomerular structures may expose intracellular tau to the immune system,
257 potentially breaking tolerance and triggering the emergence of natural or low-affinity IgG autoan-

258 tibodies against tau. Renal dysfunction may also impair clearance of circulating antibodies or im-
259 mune complexes, allowing even normally subclinical reactivity to become detectable. If the asso-
260 ciation between tau autoantibodies and kidney/urinary disease is epiphenomenal rather than causal
261 these autoantibodies may represent useful biomarkers of these diseases. Therefore, it will be im-
262 portant to monitor renal and urinary function in the current clinical trials of tau immunotherapy
263 (38-40).
264 Recent studies have explored the use of tau measurements in plasma as biomarkers for AD diag-
265 nosis and for monitoring its progression (9-12, 32, 41-45) However, we found that anti-MTBD-
266 tau autoantibodies could hinder tau detection in plasma by binding to epitopes recognized by com-
267 mercial biomarker immunoassays. The extent of this interference likely depends on both the
268 epitopes present and the design of the diagnostic assay, varying with the specific tau analytes tar-
269 geted in the assay and the particular epitopes recognized by the patients' autoantibodies. This
270 aligns with prior research indicating that both plasma anti-tau autoantibodies and administered
271 anti-tau antibodies can influence the dynamics of tau levels in plasma (46). Additionally, a recent
272 community cohort study using an immunoassay for AD screening revealed associations between
273 plasma tau levels and numerous comorbidities, with chronic kidney disease showing one of the
274 strongest associations (47). These results imply that the presence of anti-tau autoantibodies in
275 plasma might impact the effectiveness of plasma tau as an AD biomarker. This consideration may
276 become crucial as plasma tau levels move toward routine clinical use in AD diagnosis.
277
278 **Limitations**

279 Our large-scale assessment of plasma tau autoimmunity has certain limitations. Firstly, most sam-
280 ples analyzed in our study came from a university hospital cohort, implying a bias towards com-
281 plex pathologies and polymorbidities. To account for this, we included a vast collection of samples
282 from healthy blood donors. Secondly, our study is confined to two sites within a single region with
283 approximately 1,500,000 inhabitants whose ethnic composition was not thoroughly examined. Ad-
284 ditionally, a direct comparison of the prevalence of plasma anti-tau antibodies in these two cohorts
285 may potentially suffer from variations in materials, collection methods (e.g. addition of heparin
286 that may cause aggregation of MTBD-tau), and handling processes at the two different sites.
287 Thirdly, our study is restricted to the analysis of specific disease groups, the absence of an inde-
288 pendent replication cohort and the lack of a longitudinal disease design. These constraints restrict
289 our ability to verify our findings, assess temporal dynamics and the origin of these autoantibodies,
290 and explore potential causal relationships, including reverse causality, such as the presence of tau
291 antibodies in patient cohorts with renal diseases. Fourthly, the detected anti-tau antibodies may
292 crossreact with proteins expressed in the kidney or urinary tract, which could contribute to the
293 observed association with kidney and urinary disorders. To explore this possibility, we performed
294 an *in silico* analysis using BLASTP (https://blast.ncbi.nlm.nih.gov/) and compared the MTBD-tau
295 to proteins in the human kidney and urinary proteome (UniProt/Swiss-Prot). This analysis identi-
296 fied residues 368–461 of nicotinamide phosphoribosyltransferase (NAMPT) as a region with no-
297 tably high sequence identity to MTBD-tau (~28%; Supplementary Figure 4). NAMPT is a meta-
298 bolic enzyme with broad tissue distribution but relatively low expression in the kidney and urinary
299 tract (48). Nevertheless, such sequence-based analysis is limited detecting linear or conformational
300 epitopes that might mediate cross-reactivity. Furthermore, the statistical analysis of the association
301 of MTBD-tau-autoreactivity and different disorders was based on ICD-10, a medical classification

302 focused on reimbursement and cause-of-death statistics (49). We therefore performed additional
303 statistical analyses using laboratory parameters, which have provided further support for the asso-
304 ciation of tau autoimmunity and systemic disorders. Finally, we used bacterially expressed MTBD-
305 tau as target, thereby excluding full-length, other isoforms (such as big tau, a high molecular
306 weight (~110 kDa) tau isoform that includes exon 4a in the MAPT transcript (50)) or post-trans-
307 lationally modified tau epitopes, like the phosphorylated forms p-tau181 (51) and p-tau217 (52),
308 that are increasingly used as biomarkers for AD diagnosis. As a result, our methodology may miss
309 plasma anti-tau autoantibodies associated with AD pathology and could underestimate the preva-
310 lence of total anti-tau autoantibodies. Furthermore, this approach may introduce a bias towards
311 detecting autoantibodies targeting total peripheral tau which is more abundant in plasma (53).
312 Therefore, larger studies with well-powered AD patient cohorts may be needed to more robustly
313 assess the prevalence of autoantibodies selectively targeting brain-derived tau and to clarify their
314 potential association with neurodegeneration.
315

316 **Conclusions**

317 Our study identified a high seroprevalence of anti-MTBD-tau IgG autoantibodies in both plasma
318 samples from university hospital patients and healthy blood donors. Tau autoimmunity is associ-
319 ated with female sex, older age and previously unrecognized extraneural diseases. These findings
320 point to unrecognized roles for tau and anti-tau autoantibodies in extraneural pathologies.
321

322 **MATERIALS AND METHODS**

323 **METHODS**

324 **Sex as a biological variable**

325 Plasma samples from patients of both sexes were examined in this study.

326

327 **Study design**

328 From December 2017 until February 2020, residual heparin plasma samples were obtained from
329 the Department of Clinical Chemistry, University Hospital of Zurich, USZ, Switzerland. Samples
330 were collected during routine clinical care from patients admitted either as inpatients or outpatients
331 (age ≥ 18 years) and were only included if basic demographic data was available, and an informed
332 consent for research had been provided. From March until July 2020, EDTA plasma samples from
333 blood donors were obtained from the Blood Donation Center of Zurich, Switzerland, according to
334 standard criteria of blood donation. Exclusion criteria were as reported (25). Plasma samples were
335 biobanked locally and tested in an automated indirect microELISA ((25-27) and below) for natural
336 IgG autoantibodies against the MTBD-tau. Demographic and clinical data for the hospital cohort
337 was obtained from clinical records of the USZ with follow-up until December 2021, while detailed
338 clinical data for the blood donor cohort were not available for this study. ICD-10 codes (54) were
339 used for clinical data assessment. AD patients were selected using ICD-10 code F00 or G30. Non-
340 neurodegeneration controls were defined by the lack of any Fxx or Gxx ICD-10 codes.

341

342 **Automated microELISA screen**

343 Plasma samples were tested for natural anti-MTBD-tau IgG autoantibodies in a microELISA
344 screen (25-27). Briefly, high-binding 1,536-well microplates (Perkin Elmer, SpectraPlate 1536

345 HB) were coated with 1 µg/mL of recombinant MTBD-tau (37 °C, 60 min). Plates were washed
346 3x with phosphate-buffered saline 0.1% Tween®20 (PBST) using a Biotek El406 washer-dis-
347 penser and blocked with 5% milk (Migros)-PBST for 90 min. Plasma samples were diluted 1:20
348 in 1% milk-PBST and dispensed into the MTBD-tau-coated plates using ultrasound dispensing
349 with an ECHO 555 Liquid Handler (Labcyte/Beckman Coulter). Each sample was tested at eight
350 serial two-fold dilutions (1:50 to 1:6,000) using different volumes to a final volume of 3 µL/well.
351 Human IgG-depleted serum (MyBioSource) was used as negative and anti-tau RD4 (4-repeat iso-
352 form) mouse monoclonal antibody (30) (05-804 clone 1E1/A6 Merck Millipore) as positive con-
353 trol. Plates were incubated for 120 min at room temperature (RT) and washed 5x with PBST.
354 Secondary antibody peroxidase AffiniPure® goat anti-mouse IgG H+L (115-035-003, Jackson
355 ImmunoResearch) 1:2,000 diluted in 1% milk-PBST for the RD4 positive control, peroxidase Af-
356 finiPure® goat anti-human IgG Fcγ-specific (109-035-098, Jackson ImmunoResearch) 1:4,000
357 diluted in 1% milk-PBST for the plasma samples and the IgG-depleted serum negative control
358 were dispensed into the plates using a Biotek MultifloFX dispenser. Plates were incubated for 60
359 min, at RT and washed 3x with PBST. 3,3',5,5'-Tetramethylbenzidine (TMB) Chromogen Solution
360 for ELISA (Invitrogen) was added as colorimetric horseradish peroxidase (HRP) substrate for 3
361 min at RT. Finally, 0.5 M $H_2SO_4$ was added to stop the reaction. Plates were briefly centrifuged
362 after each dispensing step except after dispensing of TMB. Plates were read at Optical Density =
363 450 nm ($OD_{450nm}$) in a plate reader (Perkin Elmer, Envision).
364 For the replicability assessment, 308 samples were tested in duplicates, running the replicates on
365 the same day but using different 1536-well assay (destination) plates, different plate coordinates
366 for each replicate, and calculating the $-\log_{10}(EC_{50})$ of each replicate independently.

367 Non-specific cross-reactivity was assessed by testing plasma samples against MTBD-tau and am-
368 yloid-ß pyroglutamate (13,099 hospital patients' plasma samples) and the cellular prion protein
369 ($PrP^C$) (12,297 hospital patients' samples) using a similar protocol as described above.
370

371 **Production and purification of recombinant tau**

372 The gene encoding the human truncated 4R-tau corresponding to MTBD-tau was cloned into a
373 pRSET-A plasmid (Invitrogen) and expressed in *E.coli* BL21(DE3) cells. Cultures were grown in
374 Luria Broth (LB, Invitrogen) at 37 °C, induced with 1 mM isopropyl-β-D-thiogalactoside (IPTG)
375 at an $OD_{600}$ of 0.8 and grown for additional 6 h at 37 °C before harvesting by centrifugation
376 (6,000*g*, 10 min, 4 °C). Pellets were suspended and sonicated (30 min, 4 °C) in 20 mM piperazine-
377 N,N-bis(2-ethanesulfonic) acid (PIPES), pH 6.5, 1 mM ethylenediaminetetraacetic acid (EDTA)
378 and 50 mM 2-mercaptoethanol and. After addition of NaCl to a final concentration of 500 mM ,
379 samples were boiled (95 °C, 20 min) and centrifuged (9,000*g*, 30 min, 4 °C). Ammonium sulfate
380 was slowly added to a final concentration of 55% m/v and the suspension was stirred (1 h, room
381 temperature (RT)). Samples were centrifuged (15,000*g*, 10 min, 4 °C), pellets were resuspended
382 in 20 mM 4-(2-hydroxyethyl)piperazine-1-ethanesulfonic acid (HEPES), pH 7.0, 2 mM dithio-
383 threitol (DTT), passed through a 0.45 µm Acrodisc® filter (Sigma) and loaded onto Sepharose SP
384 Fast Flow resin (Cytiva). Tau was eluted using a linear salt gradient from 0 to 1 M NaCl in 20 mM
385 HEPES, pH 7.0, 2 mM DTT. Fractions containing tau were concentrated using Amicon® Ultra-
386 15 centrifugal filter unit (10-kDa MWCO, Merck) and dialyzed overnight at 4°C against phos-
387 phate-buffered saline (PBS, pH 7.4, Kantonsapotheke Zurich), 1mM DTT. Pooled samples were
388 passed through a HiLoad 26/60 Superdex75 (GE Healthcare) column. Protein samples were ana-
389 lyzed by SDS-PAGE and samples containing tau were concentrated using an Amicon® Ultra-15

390 centrifugal filter unit (10-kDa MWCO). Samples were assessed by SDS-PAGE and electrospray
391 ionization-mass spectrometry. Pure MTBD-tau samples were stored until further use at -80°C. The
392 concentration of tau was determined using a bicinchoninic acid assay (Pierce BCA Protein Assay
393 Kit, Thermo Fisher).
394 For the purification of full-length tau, a similar protocol was used with the following changes. The
395 gene encoding the longest 4R isoform of human full-length tau protein, $tau^{441}$, (tau/pET29b,
396 Addgene #16316, gift from Peter Klein (55)) was cloned into a pRSET-A plasmid (Invitrogen).
397 For protein expression, E.*coli* BL21(DE3)pLysS cells were transformed with the pRSET-A plas-
398 mid encoding $tau^{441}$. Cells were grown in Overnight Express™ Instant TB media (Novagen) for 6
399 h at 37 °C and then for 12 h at 25 °C. Fractions containing full-length tau were concentrated using
400 Amicon® Ultra-15 centrifugal filter unit (30-kDa MWCO, Merck).
401
402 **Purification of anti-tau autoantibodies from patient samples**
403 Heparin plasma (3- 20 mL) was diluted 1:3.3 in PBS, and centrifuged at 6,000 *g* for 10 min at 4
404 °C. The supernatant was loaded onto 3 mL of epoxy-MTBD-tau (prepared by overnight incubation
405 of MTBD-tau and epoxy resin in 0.1 M $NaH_2PO_4$–NaOH, 1 M NaCl, pH 9.2) by repetitive loading
406 of the plasma sample overnight at 4 °C. After washing with 50 mL of PBS, MTBD-tau autoanti-
407 bodies were eluted 4x with 5 mL 0.1 M glycine–HCl, pH 2.5, and immediately neutralized to pH
408 7.0 with 1 M Tris-HCl, pH 8.5. Anti-MTBD-tau antibody-containing fractions were identified by
409 indirect ELISA and concentrated stepwise using Amicon® Ultra-15, Ultra-4, and Ultra-0.5 mL
410 centrifugal filter units (50-kDa MWCO) up to a volume of 1 mL
411
412 **Competitive ELISA**

413 For the competitive sandwich ELISAs for the detection of tau, high-binding 384-well plates (Per-
414 kin Elmer, SpectraPlate 384 HB) were coated with 4 µg/mL BT2 tau monoclonal antibody
415 (#MN1010, Thermo Fisher) in PBS. Recombinant human $tau^{441}$ (rPeptide) was diluted to a final
416 concentration of 0.015 ng/mL and incubated with purified anti-tau autoantibodies four-fold serially
417 diluted (1:1.66 to 1:106.6) in 1:2 plasma under rotation at 500 rpm for 120 min at 37°C. Samples
418 were transferred to BT2-coated plates and incubated for 45 min at RT. After washing 4x with
419 PBST, plates were incubated with ab64193 (polyclonal IgG antibody; Abcam, 0.125 µg/mL) for
420 45 min at RT. Plates were washed 4x with PBST and incubated with peroxidase AffiniPure® goat
421 anti-Rabbit IgG (H+L, 111-035-045, Jackson ImmunoResearch, at a 1:2,000 dilution for 60 min
422 at RT. Plates were washed 4x with PBST and 1-Step™ Ultra TMB-ELISA solution (Thermo
423 Fisher) was added for 7 min at RT. After addition of 0.5 M $H_2SO_4$, plates were read at $OD_{450}$ nm
424 in a plate reader (Perkin Elmer, Envision).
425 For the competitive ELISAs of MTBD-tau autoantibodies, high-binding 384-well plates were
426 coated with 20 µL of 0.5 µg/mL of MTBD-tau overnight at 4 °C. Afterwards, plates were washed
427 3x with PBST and blocked with 5% SureBlock™ (Lubio) in PBST for 120 min. Purified autoan-
428 tibodies from hospital cohort patients' plasma were diluted 1:50 in 1% SureBlock™ in PBST
429 (sample buffer) and the anti-tau RD4 mouse monoclonal antibody to a final concentration of 0.4
430 µg/mL. Bovine serum albumin (BSA, Thermo Scientific), in house purified recombinant MTBD-
431 tau, a pool of eight synthetic peptides covering the sequence of MTBD-tau with 25 amino acids
432 length and 10 amino acids of overlap (Genscript) and an unrelated 25 amino acid length synthetic
433 TREM2 (Triggering receptor expressed on myeloid cells 2) peptide (GenScript) were used as com-
434 peting antigens. Antibody samples were incubated overnight at 4°C with serial 2-fold dilutions of
435 antigen solutions in sample buffer, ranging from 20,000 nM to 2.44 nM. The antibody-antigen

436 mixtures were then added to the plates and incubated for 45 min at RT. Plates were washed three
437 times with PBST, followed by the addition of secondary antibodies: peroxidase AffiniPure® goat
438 anti-Human IgG (H+L) (109-035-088, Jackson ImmunoResearch) at 1:3,000 dilution and peroxi-
439 dase AffiniPure® goat anti-mouse IgG H+L (115-035-003, Jackson ImmunoResearch) at 1:2,000
440 dilution. Secondary antibodies were incubated for 60 min at RT and plates were then washed 4x
441 with PBST. TMB Chromogen Solution for ELISA (Invitrogen) was added to the plates and incu-
442 bated for 7 min at RT. After addition of 0.5 M $H_2SO_4$, plates were read at $OD_{450nm}$ in a plate reader
443 (SpectraMax® Paradigm®, Molecular Devices).
444
445 **Indirect ELISAs**
446 To test for polyreactivity, purified anti-tau autoantibodies were tested by indirect ELISA against
447 several antigens (56, 57). High-binding 384-well plates were coated overnight at 4°C with 20 µL
448 of 1 µg/mL of MTBD-tau, 10 µg/mL of DNA from calf-thymus (Sigma), 10 µg/mL of lipopoly-
449 saccharides from E.*coli* O111:B4 (Sigma), 5 µg/mL of human insulin (Sigma), 10 µg/mL of BSA,
450 2 µg/mL of cardiolipin solution from bovine heart (Sigma) or left uncoated. Plates were washed
451 3x with PBST and then blocked in 5% SureBlock™ (Lubio) in PBST for 120 min at RT. Patient
452 purified anti-MTBD-tau autoantibodies were diluted 1:33, IgG-depleted plasma (BioSource) 1:50
453 diluted and used as negative control, anti-DNP (Sigma) diluted to 6 µg/mL, anti-tau RD4 to 6
454 µg/mL, and pooled plasma from 20 patients diluted 1:25 in 1% SureBlock™ in PBST as positive
455 controls. Samples were serially diluted 12 times 1:1 with 1% SureBlock™ in PBST in the referred
456 plates. Samples were incubated for 120 min at RT and washed 4x with PBST. 20 µL/well of sec-
457 ondary antibodies diluted in 1%SureBlock™ in PBST were added as follows: peroxidase Affini-
458 Pure® goat anti-human IgG (H+L) (109-035-088, Jackson ImmunoResearch) diluted 1:3,000 and

459 added to purified MTBD-tau autoantibodies and IKC pool wells, peroxidase AffiniPure® goat
460 anti-mouse IgG H+L (115-035-003, Jackson ImmunoResearch) at 1:2,500 dilution and added to
461 anti-RD4 wells, and peroxidase AffiniPure® goat anti-rabbit IgG (H+L) (111-035-045, Jackson
462 ImmunoResearch) at 1:4,000 dilution and added to anti-DNP wells. Plates were then washed 3x
463 with PBST. 20 µL of TMB Chromogen solution for ELISA (Invitrogen) was added and incubated
464 for 5 min at RT. After addition of 0.5 M $H_2SO_4$, plates were read at $OD_{450nm}$ in a plate reader
465 (SpectraMax® Paradigm®, Molecular Devices). For relative affinity measurements, we used an
466 indirect ELISA in 384-well plates (Perkin Elmer, SpectraPlate 384 HB) with MTBD-tau as a coat-
467 ing antigen using the following parameters: The starting concentration of all antibodies, assayed
468 in triplicates, was 10 µg/mL. They were successively diluted 1:3 to reach a concentration of $2x10^{-}$
469 $^{6}$ µg/mL. As reference antibody, we used purified RD4 kindly provided by Prof. Rohan de Silva
470 (UCL Queen Square Institute of Neurology, London, UK). As additional controls, we used anti-
471 LAG3 antibody Relatlimab (*23*), $\alpha\tau^{-}$ plasma sample and uncoated plates. The respective $EC_{50}$ val-
472 ues were then determined using logistic regression, as above, and the curves as well as the dots
473 were visualized.
474 For IgG subclassing, the following secondary antibodies were used: rabbit anti-human IgG1 (SA5-
475 10202, Invitrogen), rabbit anti-human IgG2 (SA5-10203, Invitrogen), rabbit anti-human IgG3
476 (SA5-10204, Invitrogen) or rabbit anti-human IgG4 (SA5-10205, Invitrogen) at 1:1,500 dilution,
477 peroxidase AffiniPure® goat anti-rabbit IgG (H+L) antibody (111-035-045, Jackson Immu-
478 noResearch) at 1:2,500 dilution.

479 For immunoglobulin light chain typing, the following secondary antibodies were used: Goat anti-
480 Human Kappa-HRP (19) and Goat anti-Human Lambda-HRP (19) at 1:4,000 dilution and peroxi-
481 dase AffiniPure® goat anti-mouse IgG H+L (115-035-003, Jackson ImmunoResearch) at 1:2,500
482 dilution.
483 For the epitope mapping experiments, a similar approach was used in which high-binding 384-
484 well plates were coated with 20 µL of 1 µg/mL of each MTBD-tau peptide (GenScript) in PBS
485 overnight at 4°C. Plasma samples and human IgG-depleted serum (MyBioSource) used as negative
486 control were diluted 1:50 and anti-tau RD4 mouse monoclonal antibody used as positive control
487 (05-804 clone 1E1/A6 Merck Millipore) was diluted to a final concentration of 6 µg/mL in 1%
488 SureBlock™ in PBST. The following secondary antibodies were used: peroxidase AffiniPure®
489 goat anti-human IgG (H+L) (109-035-088, Jackson ImmunoResearch) at 1:5,000 dilution and pe-
490 roxidase AffiniPure® goat anti-mouse IgG H+L (115-035-003, Jackson ImmunoResearch) at
491 1:2,500 dilution.
492 For data analysis of IgG subclassing, immunoglobulin light chain typing and epitope mapping
493 experiments, samples were considered reactive when the $OD_{450nm}$ was higher than the average of
494 all negatives $OD_{450nm}$ + 2x the standard deviation of the $OD_{450nm}$ of the negatives.
495

496 **Western blotting**

497 SH-SY5Y wild-type (Sigma) and cells overexpressing double-mutated tauP301L/S320F were
498 lysed in 0.5% Triton™ X-100 (Sigma Aldrich) in PBS, supplemented with cOmplete™ Mini
499 EDTA-free Protease Inhibitor Cocktail (Roche) on ice and supernatant was recovered after cen-
500 trifugation at 14,000g for 20 min at 4°C. Protein concentration was determined using a bicincho-
501 ninic acid assay (Pierce BCA Protein Assay Kit, Thermo Fisher) and sample volumes were adapted

502 to 30 µg of total protein. Samples were loaded onto NuPAGE 12% Bis-Tris gels (Invitrogen) and
503 blotted to nitrocellulose membranes (Invitrogen) using a dry iBlot 2 Gel Transfer Device (Invitro-
504 gen, Thermo Fisher). Membranes were cut vertically along the protein ladder and blocked with
505 5% SureBlock in PBST at 30 min for RT and incubated overnight at 4°C with patient purified anti-
506 MTBD-tau autoantibodies diluted 1:100 in 1% SureBlock, PBST. Anti-tau RD4 mouse monoclo-
507 nal antibody diluted 1:4,000 in was used a positive control. Monoclonal mouse anti-actin clone C4
508 (MAB1501R, Chemicon) diluted 1:10,000 was used as a loading control. Negative control mem-
509 branes were not incubated with primary antibodies. Membranes were washed 3x for 5 min with
510 PBST and incubated with the following secondary antibodies for 60 min at RT: peroxidase Affin-
511 iPure® goat anti-mouse IgG (H+L) (115-035-003, Jackson ImmunoResearch) and peroxidase Af-
512 finiPure® goat anti-human IgG (H+L) (109-035-088, Jackson ImmunoResearch) 1:10,000 diluted.
513 Membranes were washed 4x for 5 min with PBST and developed using the Immobilon Crescendo
514 HRP Substrate (Millipore). Imaging was performed with the Fusion SOLO S imaging system (Vil-
515 ber).
516
517 **Immunofluorescence**
518 SH-SY5Y cells were transfected with pRK5-EGFP-0N4Rtau plasmid (Addgene # 46904, a kind
519 gift of Dr Karen Ashe (48)) using Lipofectamine® 2000 according to manufacturer's protocol.
520 After 48 h cells were fixed with 4% paraformaldehyde for 20 min at RT, permeabilized with 0.5%
521 BSA, 0.1% Triton™X-100 in PBS for 20 min at RT and blocked with 0.5% BSA in PBS for 60min
522 at RT. For the immunocytochemical assays, 1:25 purified ani-MTBD-tau autoantibodies diluted
523 in 0.5% BSA in PBS were incubated with the cells for 60 min. Tau mouse monoclonal antibody
524 HT7 (MN1000 Thermo Fisher Scientific) diluted 1:500 was used as a positive control. Cells were

525 washed 3x with 0.5% BSA in PBS and incubated for 30 min at RT with: goat anti-mouse IgG
526 (H+L) cross-adsorbed Alexa Fluor ™ 555 (A-21422 Invitrogen) diluted 1:500 and counterstained
527 with 4,6-diamidino-2-phenylindole (DAPI) 1 mg/mL (Thermo Fisher) diluted 1:10,000 in 0.5%
528 BSA in PBS, and for human antibody and negative control stains with biotin AffiniPure® goat
529 anti-human IgG (H+L) (109-065-003, Jackson ImmunoResearch) diluted 1:200 in 0.5% BSA in
530 PBS. Samples were 3x washed with 0.5% BSA in PBS. For human antibody stains, samples were
531 further incubated for 30 min at RT with streptavidin Alexa Fluor™ 594 conjugate diluted 1:200
532 and counterstained with DAPI diluted 1:10,000 in 0.5% BSA in PBS. Cells were mounted on glass
533 slides with Fluorescence Mounting Medium (Thermo Fisher Scientific) and imaged using a Leica
534 TCS SP5 confocal laser scanning microscope. Imaging was performed with equipment maintained
535 by the Center for Microscopy and Image Analysis, University of Zurich.
536

537 ***In vitro* MTBD-tau aggregation assay**

538 MTBD-tau *in vitro* aggregation experiments were performed as previously described (31). Briefly,
539 7 µM of in-house purified recombinant MTBD-tau, 3.5 µM of heparin (Santa Cruz Biotechnology)
540 and 10 µM of thioflavin T (ThT, Sigma) were diluted in PBS. The patient purified anti-tau auto-
541 antibodies and controls (plasma sample reactive against the LAG3 and IgG-purified using Protein
542 G Sepharose (Cytiva)) were added at the indicated apparent stoichiometries in Figure 3. The mix-
543 tures with a total volume of 200 µl were added to black 96-well polystyrene microplates (Nunc,
544 Prod. No. 265301) and ThT fluorescence (450/480 nm ex/em filters; bottom read mode) was meas-
545 ured at 37°C under continuous orbital shaking (425 cpm) every 15 min for 96 h using a FLUOstar
546 Omega microplate reader (BMG Labtech). The mean baseline fluorescence values were sub-

547 tracted from the mean fluorescence values at each time point which were then normalized to max-
548 imum baseline-subtracted fluorescence values and multiplied by 100 (58).
549
550 **Statistical analysis**
551 Antibody titers were defined as the negative logarithm half-maximal responses ($-\log_{10}(EC_{50})$) ob-
552 tained by fitting the $OD_{450nm}$ of the eight dilution points of each sample tested in the microELISA
553 to a logistic regression fitter. We classified as positives samples with a cut-off of $-\log_{10}(EC_{50}) \geq 1.8$
554 (25), corresponding to a nominal dilution of > 1/64. Non-informative samples (fitting error >20%
555 $-\log_{10}(EC_{50})$ or high background) were excluded from the analysis (25). In cases where more than
556 one sample was available for the same individual the most recent $\log_{10}(EC_{50})$ value was used.
557 Age is presented as median with interquartile range (IQR) and comparisons were performed using
558 non-parametric Mann-Whitney U test. Categorized age groups and sex of positives and negatives
559 are shown as percentages and compared using two-proportions Z-test or $\chi^2$ test for trend in propor-
560 tions. Log-binomial regression models (28, 59) using MTBD-tau autoreactivity were employed to
561 estimate age-and-sex adjusted RRs (aRR) and 95% confidence intervals (CIs), and to investigate
562 the association between the detection of anti-MTBD-tau IgG autoantibodies and different demo-
563 graphic features.
564 For the AD cohort microELISA screen, $\log_{10}(EC_{50})$ values were compared using Mann-Whitney
565 U test. Additionally, Bayesian logistic regression was conducted (25, 60-62), using $-\text{logit}_{10}(EC_{50})$
566 values as outcome, i.e. without dichotomising the outcome using the R package rstanarm and the
567 following priors (prior=normal[0, 2.5, autoscale=TRUE],prior_intercept = normal[5000, 2.5, au-
568 toscale=TRUE)] prior_aux = exponential [1, autoscale =TRUE]. We aimed to confirm the positive
569 association between ICD-10 codes previously identified using a conventional logistic regression

570 model with high $-\log_{10}(EC_{50})$ values. Each ICD-10 code was analyzed in an independent logistic
571 regression and adjusted for age and sex.
572 The association between MTBD-tau-autoreactivity and neurological and systemic disorders, re-
573 spectively, was analysed by applying multivariate log-binomial regression models to estimate
574 aRRs and 95% CIs. For neurological disorders, 23 major groups of ICD-10 codes (Supplemental
575 Table 3) corresponding to neurological disorders identified at least once in the positive samples
576 were used. For systemic disorders, the 27 major groups of ICD-10 codes (Supplemental Table 4)
577 or 276 individual ICD-10 codes corresponding to systemic disorders identified at least once in the
578 positive samples and with at least 200 total counts were used to avoid overinterpretation of rare
579 cases of disease. Individual disease entities with a P value $< 0.05$ Bonferroni corrected for multiple
580 comparisons were included in a multivariate log-binomial regression analysis.
581 For the association between MTBD-tau-autoreactivity and clinical laboratory parameters, we used
582 laboratory parameters with more than 2,000 total counts and calculated median values of the total
583 values available for each patient in case of repetition of the clinical laboratory test. We used mul-
584 tivariate log-binomial regression models to estimate aRR and 95% CI using 106 clinical laboratory
585 tests.
586 Statistical significance was defined by 2-tailed P-value $\leq 0.05$. Statistical analyses and data visu-
587 alization were performed using R version 4.3.2 and RStudio version 1.4.1106 (63).
588

589 **Study approval**

590 Collection of samples and clinical data were conducted according to study protocols approved by
591 the Cantonal Ethics Committee of the Canton of Zurich, Switzerland (KEK-ZH Nr. 2015-0561,
592 BASEC-Nr. 2018-01042, and BASEC-Nr. 2020-01731).

593

594 **Data availability:**

595 Data and material requests should be addressed to the corresponding authors. Materials will be

596 shared upon approval by an ethics committee or review board and a material transfer agreement.

597

598 **List of Supplementary Materials:**

599 Supplemental Figure 1, 2, 3 and 4

600 Supplemental Table 1, 2, 3 and 4

601

602 **References**


603 1. Gu Y, Oyama F, and Ihara Y. Tau is widely expressed in rat tissues. *J Neurochem.*
604 1996;67(3):1235-44.
605 2. Uhlen M, Fagerberg L, Hallstrom BM, Lindskog C, Oksvold P, Mardinoglu A, et al.
606 Proteomics. Tissue-based map of the human proteome. *Science.*
607 2015;347(6220):1260419.
608 3. Sotiropoulos I, Galas MC, Silva JM, Skoulakis E, Wegmann S, Maina MB, et al. Atypical,
609 non-standard functions of the microtubule associated Tau protein. *Acta Neuropathol*
610 *Commun.* 2017;5(1):91.
611 4. Rinschen MM, Gödel M, Grahammer F, Zschiedrich S, Helmstädter M, Kretz O, et al. A
612 Multi-layered Quantitative In Vivo Expression Atlas of the Podocyte Unravels Kidney
613 Disease Candidate Genes. *Cell Rep.* 2018;23(8):2495-508.
614 5. Ho KH, Yang X, Osipovich AB, Cabrera O, Hayashi ML, Magnuson MA, et al. Glucose
615 Regulates Microtubule Disassembly and the Dose of Insulin Secretion via Tau
616 Phosphorylation. *Diabetes.* 2020;69(9):1936-47.
617 6. Kosik KS, Joachim CL, and Selkoe DJ. Microtubule-associated protein tau (tau) is a major
618 antigenic component of paired helical filaments in Alzheimer disease. *Proc Natl Acad Sci*
619 *U S A.* 1986;83(11):4044-8.
620 7. Joachim CL, Morris JH, Kosik KS, and Selkoe DJ. Tau antisera recognize neurofibrillary
621 tangles in a range of neurodegenerative disorders. *Ann Neurol.* 1987;22(4):514-20.
622 8. Hanseeuw BJ, Betensky RA, Jacobs HIL, Schultz AP, Sepulcre J, Becker JA, et al. Association
623 of Amyloid and Tau With Cognition in Preclinical Alzheimer Disease: A Longitudinal Study.
624 *JAMA Neurol.* 2019;76(8):915-24.
625 9. Mattsson N, Zetterberg H, Janelidze S, Insel PS, Andreasson U, Stomrud E, et al. Plasma
626 tau in Alzheimer disease. *Neurology.* 2016;87(17):1827-35.
627 10. Janelidze S, Mattsson N, Palmqvist S, Smith R, Beach TG, Serrano GE, et al. Plasma P-
628 tau181 in Alzheimer's disease: relationship to other biomarkers, differential diagnosis,
629 neuropathology and longitudinal progression to Alzheimer's dementia. *Nat Med.*
630 2020;26(3):379-86.
631 11. Mielke MM, Hagen CE, Wennberg AMV, Airey DC, Savica R, Knopman DS, et al. Association
632 of Plasma Total Tau Level With Cognitive Decline and Risk of Mild Cognitive Impairment
633 or Dementia in the Mayo Clinic Study on Aging. *JAMA Neurol.* 2017;74(9):1073-80.
634 12. Palmqvist S, Tideman P, Mattsson-Carlgren N, Schindler SE, Smith R, Ossenkoppele R, et
635 al. Blood Biomarkers to Detect Alzheimer Disease in Primary Care and Secondary Care.
636 *JAMA.* 2024.
637 13. Asuni AA, Boutajangout A, Quartermain D, and Sigurdsson EM. Immunotherapy targeting
638 pathological tau conformers in a tangle mouse model reduces brain pathology with
639 associated functional improvements. *J Neurosci.* 2007;27(34):9115-29.
640 14. Boutajangout A, Ingadottir J, Davies P, and Sigurdsson EM. Passive immunization targeting
641 pathological phospho-tau protein in a mouse model reduces functional decline and clears
642 tau aggregates from the brain. *J Neurochem.* 2011;118(4):658-67.
643 15. Congdon EE, and Sigurdsson EM. Tau-targeting therapies for Alzheimer disease. *Nat Rev*
644 *Neurol.* 2018;14(7):399-415.

645 16. Rothstein TL. Natural Antibodies as Rheostats for Susceptibility to Chronic Diseases in the
646 Aged. *Front Immunol.* 2016;7:127.
647 17. Lutz HU, Binder CJ, and Kaveri S. Naturally occurring auto-antibodies in homeostasis and
648 disease. *Trends Immunol.* 2009;30(1):43-51.
649 18. Bastard P, Gervais A, Le Voyer T, Rosain J, Philippot Q, Manry J, et al. Autoantibodies
650 neutralizing type I IFNs are present in ~4% of uninfected individuals over 70 years old and
651 account for ~20% of COVID-19 deaths. *Sci Immunol.* 2021;6(62).
652 19. Jaycox JR, Dai Y, and Ring AM. Decoding the autoantibody reactome. *Science.*
653 2024;383(6684):705-7.
654 20. Florance NR, Davis RL, Lam C, Szperka C, Zhou L, Ahmad S, et al. Anti-N-methyl-D-
655 aspartate receptor (NMDAR) encephalitis in children and adolescents. *Ann Neurol.*
656 2009;66(1):11-8.
657 21. Lennon VA, Wingerchuk DM, Kryzer TJ, Pittock SJ, Lucchinetti CF, Fujihara K, et al. A serum
658 autoantibody marker of neuromyelitis optica: distinction from multiple sclerosis. *Lancet.*
659 2004;364(9451):2106-12.
660 22. Ferrero J, Williams L, Stella H, Leitermann K, Mikulskis A, O'Gorman J, and Sevigny J. First-
661 in-human, double-blind, placebo-controlled, single-dose escalation study of aducanumab
662 (BIIB037) in mild-to-moderate Alzheimer's disease. *Alzheimers Dement (N Y).*
663 2016;2(3):169-76.
664 23. Bartos A, Fialová L, and Švarcová J. Lower Serum Antibodies Against Tau Protein and
665 Heavy Neurofilament in Alzheimer's Disease. *J Alzheimers Dis.* 2018;64(3):751-60.
666 24. Kronimus Y, Albus A, Balzer-Geldsetzer M, Straub S, Semler E, Otto M, et al. Naturally
667 Occurring Autoantibodies against Tau Protein Are Reduced in Parkinson's Disease
668 Dementia. *PLoS One.* 2016;11(11):e0164953.
669 25. Emmenegger M, De Cecco E, Lamparter D, Jacquat RPB, Riou J, Menges D, et al.
670 Continuous population-level monitoring of SARS-CoV-2 seroprevalence in a large
671 European metropolitan region. *iScience.* 2023;26(2):105928.
672 26. Emmenegger M, Zografou C, Yile D, Hoyt LR, Gudneppanavar R, Chincisan A, et al. The
673 Cystic Fibrosis Transmembrane Regulator Controls Tolerogenic Responses to Food
674 Allergens in Mice and Humans. *medRxiv.* 2024.
675 27. Senatore A, Frontzek K, Emmenegger M, Chincisan A, Losa M, Reimann R, et al. Protective
676 anti-prion antibodies in human immunoglobulin repertoires. *EMBO Mol Med.*
677 2020;12(9):e12739.
678 28. Diaz-Quijano FA. A simple method for estimating relative risk using logistic regression.
679 *BMC Med Res Methodol.* 2012;12:14.
680 29. Donoghoe MW, and Marschner IC. Logbin: An R Package for Relative Risk Regression
681 Using the Log-Binomial Model. *Journal of Statistical Software* 2018;86(21).
682 30. de Silva R, Lashley T, Gibb G, Hanger D, Hope A, Reid A, et al. Pathological inclusion bodies
683 in tauopathies contain distinct complements of tau with three or four microtubule-
684 binding repeat domains as demonstrated by new specific monoclonal antibodies.
685 *Neuropathol Appl Neurobiol.* 2003;29(3):288-302.
686 31. Apetri A, Crespo R, Juraszek J, Pascual G, Janson R, Zhu X, et al. A common antigenic motif
687 recognized by naturally occurring human V. *Acta Neuropathol Commun.* 2018;6(1):43.

32. Pase MP, Beiser AS, Himali JJ, Satizabal CL, Aparicio HJ, DeCarli C, et al. Assessment of Plasma Total Tau Level as a Predictive Biomarker for Dementia and Related Endophenotypes. *JAMA Neurol.* 2019;76(5):598-606.
33. Barini E, Plotzky G, Mordashova Y, Hoppe J, Rodriguez-Correa E, Julier S, et al. Tau in the brain interstitial fluid is fragmented and seeding-competent. *Neurobiol Aging.* 2022;109:64-77.
34. Dahm L, Ott C, Steiner J, Stepniak B, Teegen B, Saschenbrecker S, et al. Seroprevalence of autoantibodies against brain antigens in health and disease. *Ann Neurol.* 2014;76(1):82-94.
35. Yu G, Chen J, Xu Y, Zhu C, Yu H, Liu S, et al. Generation of goats lacking prion protein. *Mol Reprod Dev.* 2009;76(1):3.
36. Tsuboi Y, Uitti RJ, Delisle MB, Ferreira JJ, Brefel-Courbon C, Rascol O, et al. Clinical features and disease haplotypes of individuals with the N279K tau gene mutation: a comparison of the pallidopontonigral degeneration kindred and a French family. *Arch Neurol.* 2002;59(6):943-50.
37. Vallés-Saiz L, Peinado-Cahuchola R, Ávila J, and Hernández F. Microtubule-associated protein tau in murine kidney: role in podocyte architecture. *Cell Mol Life Sci.* 2022;79(2):97.
38. Congdon EE, Ji C, Tetlow AM, Jiang Y, and Sigurdsson EM. Tau-targeting therapies for Alzheimer disease: current status and future directions. *Nat Rev Neurol.* 2023;19(12):715-36.
39. ClinicalTrial.gov N, Dominantly Inherited Alzheimer Network Trial: An Opportunity to Prevent Dementia. A Study of Potential Disease Modifying Treatments in Individuals With a Type of Early Onset Alzheimer's Disease Caused by a Genetic Mutation (DIAN-TU). https://clinicaltrials.gov/study/NCT05269394?cond=Alzheimer%20Disease&term=E2814&rank=1; 2023.
40. Barton ME, Van Den Steen B, Van Tricht HLG, Byrnes W, Purcell FE, Southcott SA, et al. Update on the TOGETHER study: a patient- and investigator-blind, randomized, placebo-controlled study evaluating the efficacy, safety and tolerability of bepranemab, UCB0107, in prodromal-to-mild Alzheimer's disease. *Alzheimer's & Dementia.* 2022;18(S10):e068973.
41. Moscoso A, Grothe MJ, Ashton NJ, Karikari TK, Lantero Rodríguez J, Snellman A, et al. Longitudinal Associations of Blood Phosphorylated Tau181 and Neurofilament Light Chain With Neurodegeneration in Alzheimer Disease. *JAMA Neurol.* 2021;78(4):396-406.
42. Barthélemy NR, Li Y, Joseph-Mathurin N, Gordon BA, Hassenstab J, Benzinger TLS, et al. A soluble phosphorylated tau signature links tau, amyloid and the evolution of stages of dominantly inherited Alzheimer's disease. *Nat Med.* 2020;26(3):398-407.
43. Karikari TK, Pascoal TA, Ashton NJ, Janelidze S, Benedet AL, Rodriguez JL, et al. Blood phosphorylated tau 181 as a biomarker for Alzheimer's disease: a diagnostic performance and prediction modelling study using data from four prospective cohorts. *Lancet Neurol.* 2020;19(5):422-33.
44. Park JC, Han SH, Yi D, Byun MS, Lee JH, Jang S, et al. Plasma tau/amyloid-β1-42 ratio predicts brain tau deposition and neurodegeneration in Alzheimer's disease. *Brain.* 2019;142(3):771-86.

732 45. Palmqvist S, Janelidze S, Quiroz YT, Zetterberg H, Lopera F, Stomrud E, et al. Discriminative
733 Accuracy of Plasma Phospho-tau217 for Alzheimer Disease vs Other Neurodegenerative
734 Disorders. *JAMA.* 2020;324(8):772-81.
735 46. Yanamandra K, Patel TK, Jiang H, Schindler S, Ulrich JD, Boxer AL, et al. Anti-tau antibody
736 administration increases plasma tau in transgenic mice and patients with tauopathy. *Sci*
737 *Transl Med.* 2017;9(386).
738 47. Mielke MM, Dage JL, Frank RD, Algeciras-Schimnich A, Knopman DS, Lowe VJ, et al.
739 Performance of plasma phosphorylated tau 181 and 217 in the community. *Nat Med.*
740 2022;28(7):1398-405.
741 48. https://www.proteinatlas.org/ENSG00000105835-NAMPT/tissue.
742 49. St Germaine-Smith C, Metcalfe A, Pringsheim T, Roberts JI, Beck CA, Hemmelgarn BR, et
743 al. Recommendations for optimal ICD codes to study neurologic conditions: a systematic
744 review. *Neurology.* 2012;79(10):1049-55.
745 50. Fischer I. Big Tau: What We Know, and We Need to Know. *eNeuro.* 2023;10(5).
746 51. Meng J, and Lei P. Plasma pTau181 as a biomarker for Alzheimer's disease. *MedComm*
747 *(2020).* 2020;1(1):74-6.
748 52. Telser J, Risch L, Saely CH, Grossmann K, and Werner P. P-tau217 in Alzheimer's disease.
749 *Clin Chim Acta.* 2022;531:100-11.
750 53. Gonzalez-Ortiz F, Turton M, Kac PR, Smirnov D, Premi E, Ghidoni R, et al. Brain-derived
751 tau: a novel blood-based biomarker for Alzheimer's disease-type neurodegeneration.
752 *Brain.* 2023;146(3):1152-65.
753 54. Organization WH. 2004.
754 55. Hedgepeth CM, Conrad LJ, Zhang J, Huang HC, Lee VM, and Klein PS. Activation of the Wnt
755 signaling pathway: a molecular mechanism for lithium action. *Dev Biol.* 1997;185(1):82-
756 91.
757 56. Bunker JJ, Erickson SA, Flynn TM, Henry C, Koval JC, Meisel M, et al. Natural polyreactive
758 IgA antibodies coat the intestinal microbiota. *Science.* 2017;358(6361).
759 57. Mouquet H, Scheid JF, Zoller MJ, Krogsgaard M, Ott RG, Shukair S, et al. Polyreactivity
760 increases the apparent affinity of anti-HIV antibodies by heteroligation. *Nature.*
761 2010;467(7315):591-5.
762 58. Orrú CD, Yuan J, Appleby BS, Li B, Li Y, Winner D, et al. Prion seeding activity and infectivity
763 in skin samples from patients with sporadic Creutzfeldt-Jakob disease. *Sci Transl Med.*
764 2017;9(417).
765 59. McNutt LA, Wu C, Xue X, and Hafner JP. Estimating the relative risk in cohort studies and
766 clinical trials of common outcomes. *Am J Epidemiol.* 2003;157(10):940-3.
767 60. Emmenegger M, Emmenegger V, Shambat SM, Scheier TC, Gomez-Mejia A, Chang CC, et
768 al. Antiphospholipid antibodies are enriched post-acute COVID-19 but do not modulate
769 the thrombotic risk. *Clin Immunol.* 2023;257:109845.
770 61. M. Emmenegger VE, in Zenodo, 2023. https://doi.org/10.5281/zenodo.10051979. .
771 62. Losa M, Emmenegger M, De Rossi P, Schurch PM, Serdiuk T, Pengo N, et al. The ASC
772 inflammasome adapter governs SAA-derived protein aggregation in inflammatory
773 amyloidosis. *EMBO Mol Med.* 2024;16(9):2024-42.
774 63. RStudioTeam. (RStudio P, Boston, MA, 2021).

**Acknowledgments:**

The authors wish to thank the hospital patients and blood donors for their generous altruistic contributions to this study. Imaging was performed with equipment maintained by the Center for Microscopy and Image Analysis, University of Zurich, Switzerland, and electrospray ionization-mass spectrometry at the Functional Genomics Center Zurich, University of Zurich, Switzerland. We thank Prof. Rohan de Silva (UCL Queen Square Institute of Neurology, London, UK) for providing the purified anti-MTBD-tau antibody RD4. We thank Dr. Marco Losa for the generous provision of secondary antibodies for light chain typing and Magdalena Bialkowska, Lisa Caflisch, Berre Doğançay, Julie Domange, Marigona Imeri, Lorène Mottier, Rea Müller, Antonella Rosati, Dezirae Schneider, and Anne Wiedmer for help with the high-throughput assays. Insightful advice about programming in R software was provided by Reto Guadagnini.

**Funding:**

University of Zürich, Candoc grant FK-19-025 (ADM)

Swiss Personalised Health Network, SPHN, driver project grant 2017DRI17 (AA)

Swiss National Foundation SNF (SNSF grant ID 179040 and grant ID 207872, Sinergia grant ID 183563) (AA)

European Research Council ERC Prion2020, 670958 (AA)

Nomis Foundation (AA)

Innovation Fund of the University Hospital Zurich (INOV00096) (AA)

University Hospital Zurich Foundation grant USZF27101 (with contributions of the NOMIS Foundation, the Schwyzer Winiker Stiftung, and the Baugarten Stiftung, AA, ME)

HMZ ImmunoTarget grant, Stiftung Neuropath and GELU Foundation (AA)

Michael J. Fox Foundation (grant ID MJFF-020710 and MJFF-021073) (SH).

**Author contributions:**

Conceived and designed the experiments: ADM, SH, AA. Supervised the study: SH, AA. Performed tau protein purification: ADM, EDC, JG. Performed tau microELISA automated screen: ADM, ME. Performed amyloid-ß pyroglutamate and cellular prion protein microELISA automated screen: MC, KF, ME. Maintained microELISA automated platform: ME. Performed purification, validation and characterization of anti-tau autoantibodies: ADM, JG. Maintained the clinical database: ME, AC. Performed data analysis and visualization: ADM. Wrote the first draft of manuscript: ADM. Corrected and advised on subsequent versions of the manuscript: ADM, ME, SH, AA. All authors reviewed and approved the final version of the manuscript and consented to be accountable for the work.

## Figures

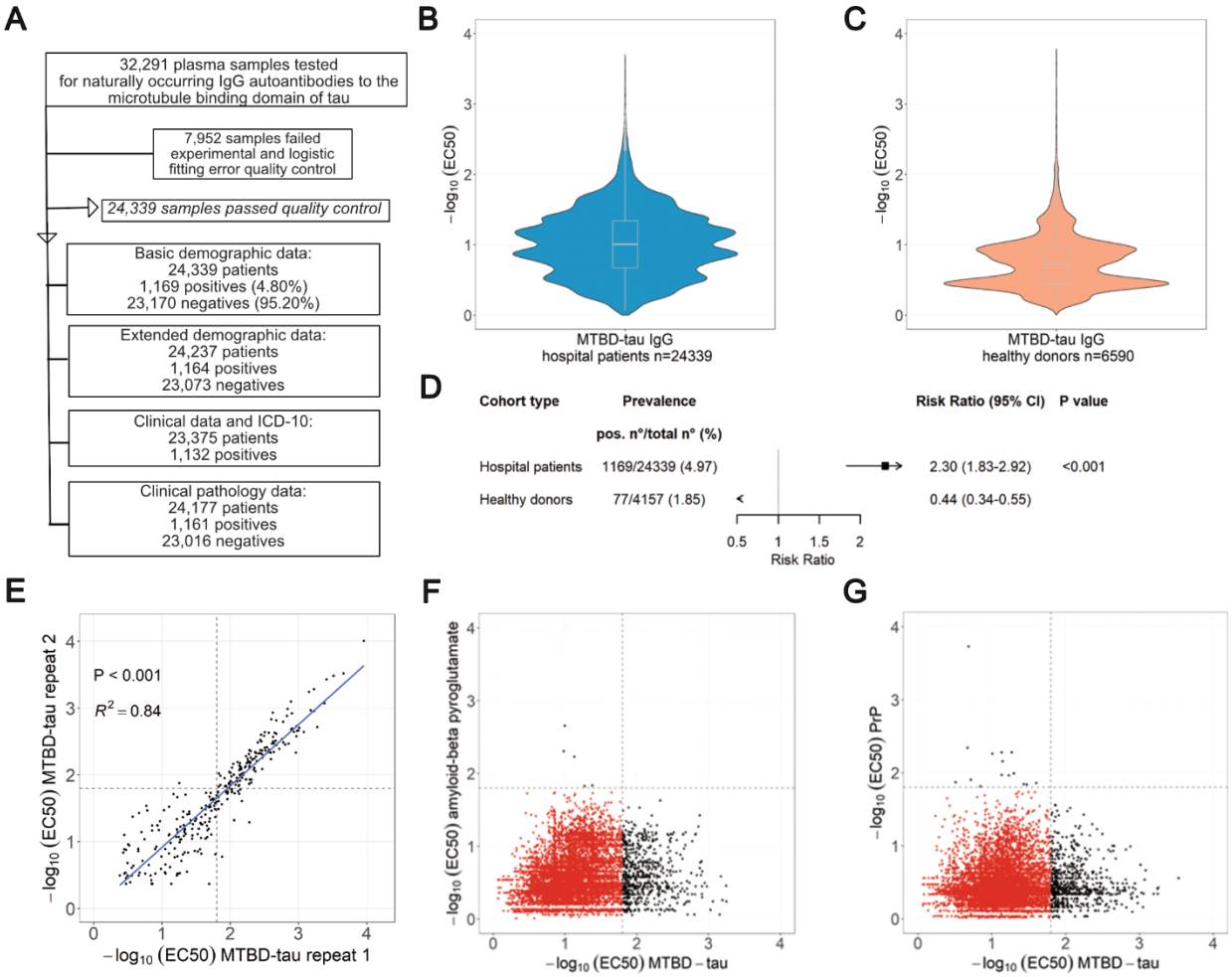


**Figure 1. Study overview and seroprevalence of anti-MTBD-tau IgG autoantibodies. A.** Flowchart of the study design. **B.-C.** Distribution of $-\log_{10}(EC_{50})$ values obtained from the micro-ELISA screen of hospital (B) and blood donor (C) plasma samples. **D.** Age- and sex-adjusted risk ratio ratios and 95% confidence intervals (CI; I bars) for the detection of anti-tau autoantibodies in hospital and blood-bank plasma samples. **E.** Replicability of microELISA duplicates with independent estimation of the $-\log_{10}(EC_{50})$ values. Dashed lines: cut-off value of $-\log_{10}(EC_{50}) = 1.8$. **F.** $-\log_{10}(EC_{50})$ values of samples tested by microELISA against MTBD-tau and amyloid-ß pyroglutamate. **G.** Same as shown in (F), but for samples tested against MTBD-tau and the cellular prion protein ($PrP^{C}$).

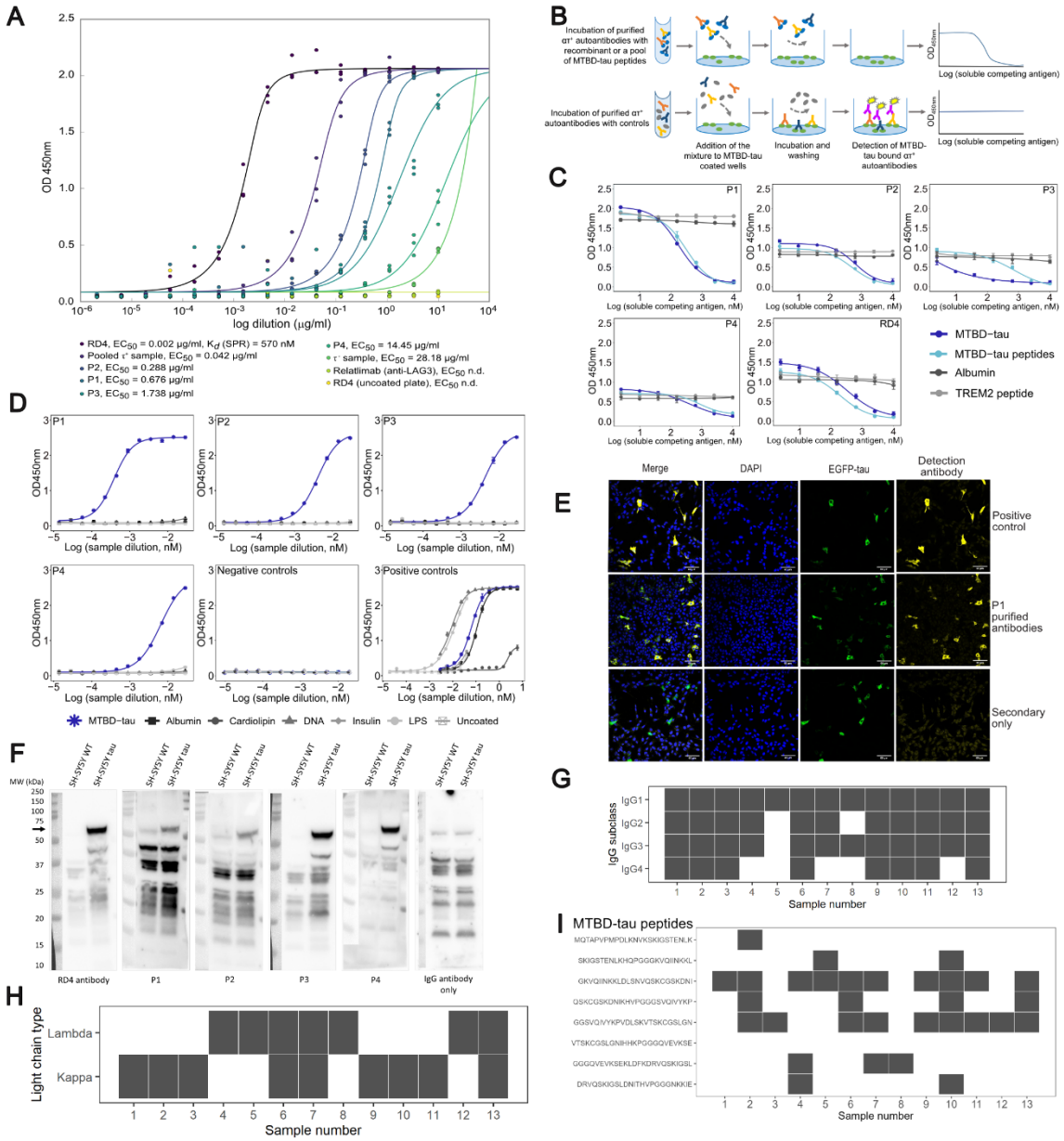


**Figure 2. Biophysical characterization of samples from ατ$^+$ patients. A**. Indirect ELISA of purified anti-MTBD-tau autoantibodies from four ατ$^+$ samples and from 6 pooled ατ$^+$ samples. All antibodies were assayed at the same concentration to compare their $EC_{50}$ to that of RD4. Relatimab (anti-LAG3) was used as negative control. $EC_{50}$ values are indicated in the Figure. n.d.: not determined. **B.** Principle of competition ELISA. **C.** Competition ELISA of purified anti-tau autoantibodies from four ατ$^+$ patients against albumin, recombinant MTBD-tau, a pool of synthetic peptides spanning the sequence of MTBD-tau and synthetic TREM2. RD4 antibody: positive control. Mean values ± SD of two replicates. **D.** Indirect ELISA to assess the reactivity of purified anti-tau autoantibodies against albumin, cardiolipin, double-stranded DNA, insulin, lipopolysaccharides

836 (LPS), MTBD-tau and uncoated plates. Positive controls were as follows: RD4 antibody for
837 MTBD-tau, anti-DNP antibody for cardiolipin, albumin and DNA and the IKC pool of 20 heparin
838 plasma samples for insulin, LPS and uncoated plates. Mean values ± SD of two replicates are
839 shown. **E.** Representative immunofluorescence images of SH-SY5Y cells expressing EGFP-
840 0N4R-tau using affinity-purified anti-tau autoantibodies. HT7 pan-tau antibody: positive control.
841 No primary antibody: negative control. Scale bar: 60 µm. **F.** Western blot of cell lysates from wild-
842 type (SH-SY5Y WT) or tau$^{P301L/S320F}$-overexpressing cells (SH-SY5Y tau) using purified anti-tau
843 autoantibodies from four $\alpha\tau^{+}$ patients. Positive control: RD4. Negative control: omission of pri-
844 mary antibody. **G.** IgG subclass typing of 13 $\alpha\tau^{+}$ plasma samples. Gray and white boxes: reactive
845 and non-reactive samples, respectively. **H.** κ/λ light chain typing of the samples in F. **I.** Epitope
846 mapping of the samples in Figure 2F against 25mer MTBD-tau peptides with 10 residues overlap.
847 Vertical axis: sequences of the MTBD-tau peptides covering the sequence of MTBD-tau.

848

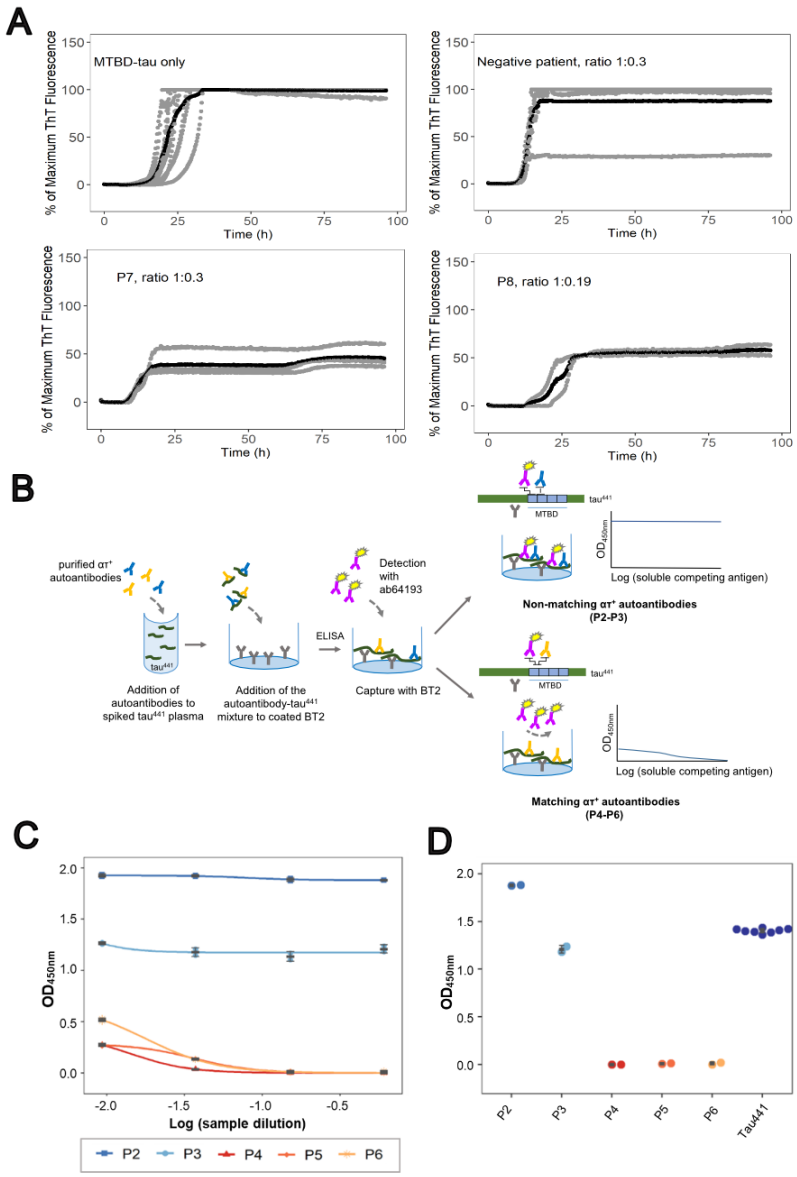


**Figure 3.** Natural ατ autoantibodies inhibit tau aggregation and impair tau detection. A. Kinetic aggregation curves of MTBD-tau followed by ThT fluorescence in the absence (n=12) or presence of purified ατ autoantibodies (patient P7 (n=4) and P8 (n=2)) or antibodies from an ατ- sample (n=6). Stoichiometric ratios as indicated. Gray lines indicate individual replicates and black lines the average of the replicates. B. Principle of the competition sandwich ELISA. C. Competitive sandwich ELISA to assess the ability of purified anti-tau autoantibodies with matching (P4-P6) and non-matching (P2 and P3) epitopes to the commercial detection antibody, ab64193, to impair

858 the detection of free tau441 spiked in plasma (dark blue). Serial dilutions of purified anti-tau anti-
859 bodies are shown in (C) and binding at highest anti-tau antibody concentrations in (D).

860

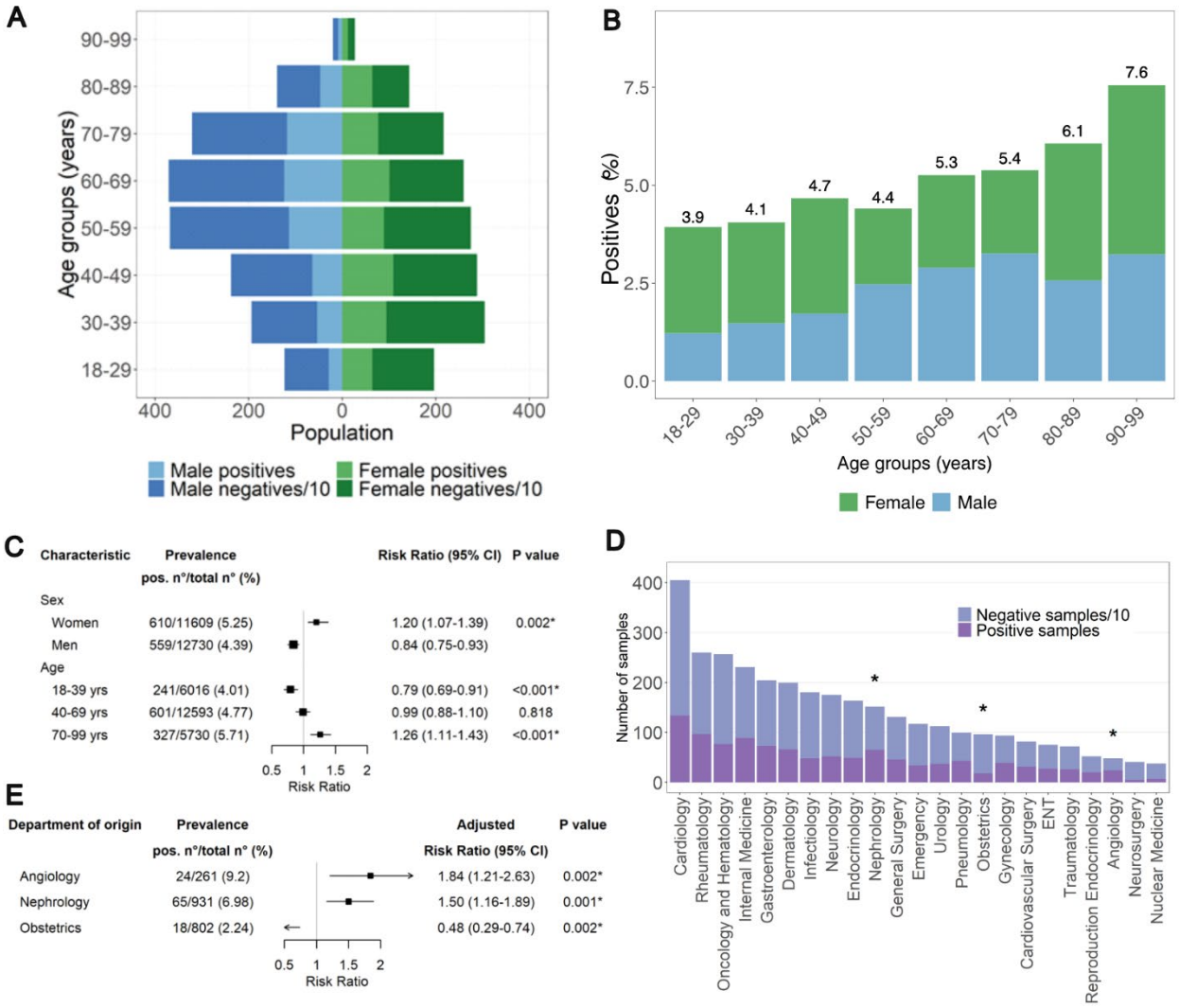


**Figure 4. Demographic characteristics of hospital patients' cohort. A.** Age and sex pyramid of positive and negative individuals. **B.** Percentage of positives among hospital patients across decadic age groups. The numbers on top of each bar correspond to the positivity rates. $\chi^2$ test for trend in proportions. **C.** RR ± 95% CI for $\alpha\tau^+$ autoantibodies according to sex and age groups. Asterisks: $P < 0.05$ after Bonferroni correction. **D.** Break-down of samples by clinical department. Asterisks: $P < 0.05$ (two-proportions z-test with Bonferroni correction). **E.** aRR ± 95% CI for $\alpha\tau^+$ samples by clinical department. Asterisks: $P < 0.05$ after Bonferroni correction.

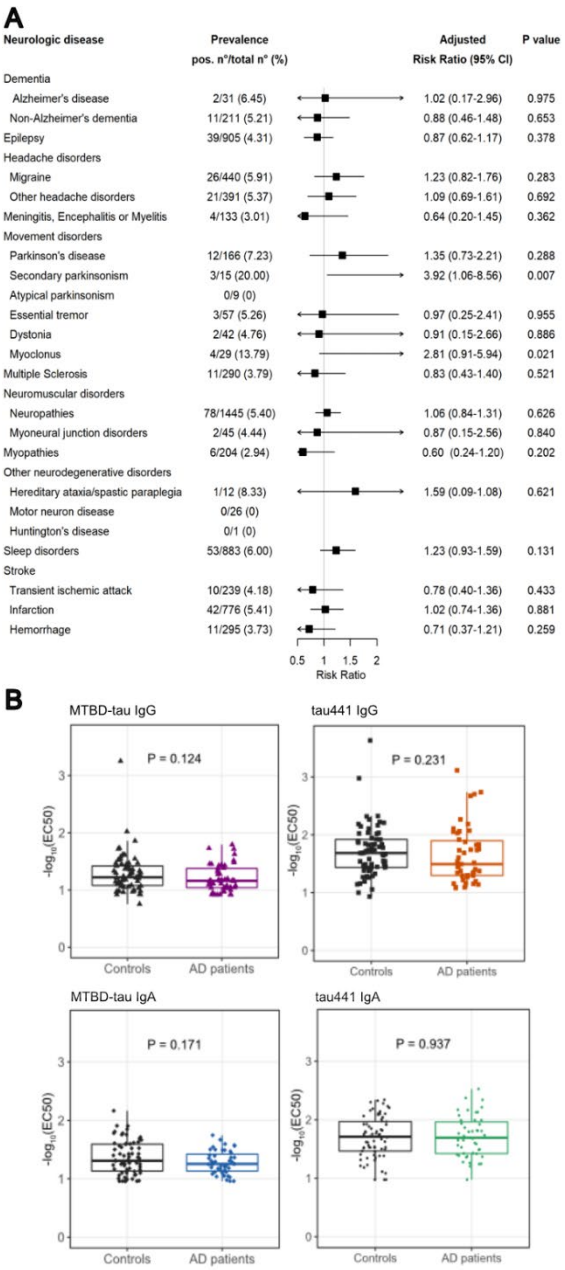


**Figure 5. aRR of MTBD-tau-autoreactivity for major groups of neurological disorders and reactivity profiles for AD screen**. **A.** aRR and 95% CI (I bars) for $\alpha\tau^{+}$ autoantibodies according to different groups of neurological disorders. No P values remained significant after Bonferroni correction. **B.** Boxplots showing the 25$^{th}$, 50$^{th}$ (median) and 75$^{th}$ percentiles of the reactivity profiles for AD and control patients (Mann-Whitney U test).

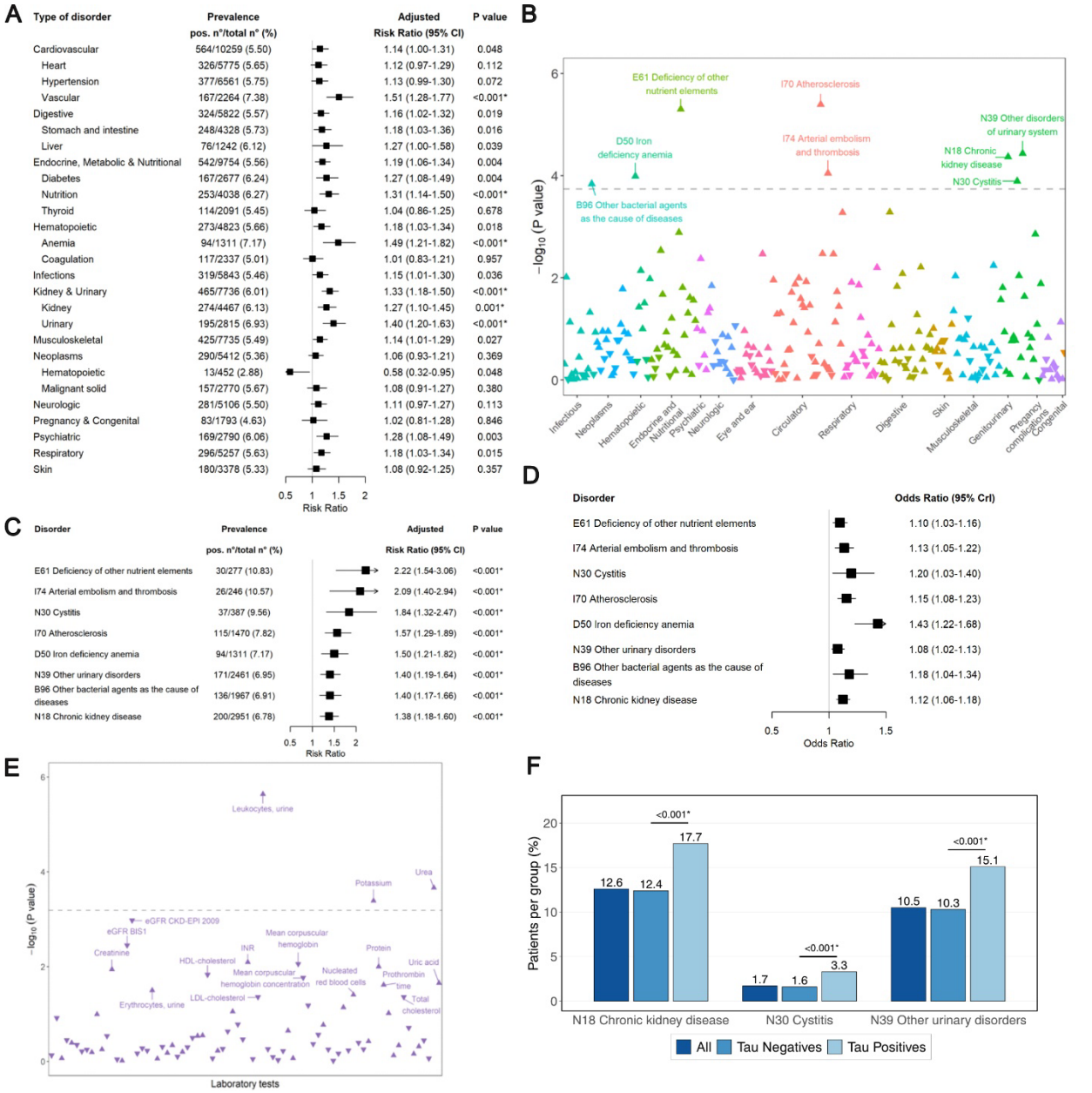


**Figure 6. Association of MTBD-tau IgG autoantibodies with systemic disorders and clinical laboratory data. A.** aRR ± 95% CI (bars) for $\alpha\tau^+$ autoantibodies grouped 27 different main systemic clinical conditions. Asterisks: $P < 0.05$ after Bonferroni correction. **B.** $-\log_{10}$(P value) of the log-binomial regression for the presence of plasma MTBD-tau IgG autoantibodies for 276 disorders according to ICD-10 codes and adjusted for age and sex. Triangles pointing upwards and downwards: positive and coefficients, respectively; gray dashed line: $P < 0.05$ after Bonferroni correction (here and henceforth). P values significant after Bonferroni adjustment are labelled with the ICD codes. **C.** Same as (A), but according to individual disease entities from (B). **D**. Bayesian

889 logistic regression adjusted for age and sex on ICD-10 codes significantly associated in B. and
890 using -$logit_{10}(EC_{50})$ as continuous outcome (odds ratio ± 95% credible intervals). This analysis
891 confirms the positive association of these ICD-10 codes with ατ reactivity (from B). **E.** $log_{10}$(P
892 value) of the log-binomial regression for the presence of plasma MTBD-tau IgG autoantibodies
893 and clinical laboratory parameters. P values significant after Bonferroni adjustment are labelled
894 with the ICD codes. The gray dashed line indicates the significance level after Bonferroni correc-
895 tion (<0.05/106=0.00047). eGFR CKD-EPI 2009: estimated glomerular filtration rate using the
896 Chronic Kidney Disease Epidemiology Collaboration 2009 equation; eGFR BIS1: estimated glo-
897 merular filtration rate using the older adults Berlin Initiative Study 1 equation. INR: international
898 normalized ratio. LDL: low-density lipoprotein. HDL: high-density lipoprotein. **F.** Calculated
899 prevalence of different ICD-10 codes in the total cohort (dark blue), $\alpha\tau^-$ (intermediate blue) and
900 $\alpha\tau^+$ samples (light blue). P-values < 0.001 (two-proportions z-test).
901
902
903
904
905
906
907
908
909
910
911
912